Optical Engineering

SPIEDigitalLibrary.org/oe

Theoretical solution for nonlinear Schrodinger equation utilized in high-power fiber laser application

Younis Mohamed Atiah Al-zahy

Theoretical solution for nonlinear Schrodinger equation utilized in high-power fiber laser application

Younis Mohamed Atiah Al-zahy*
Misan University, College of Dentistry, Department of Physics, Iraq

Abstract. An analytical solution of the generalized nonlinear Schrodinger equation which is implemented with fiber laser applications has been presented. The solution based on the exp-function method which is depending on time, space and small perturbations has been found. This solution was used to test the behavior and study the propagation characteristics of laser pulses and compared with some of the researches in the same field and the nonlinear effects as gain dispersion, second anomalous group velocity dispersion, self phase modulation, and frequency are investigated. The net results are that the parabolic pulse growth after $z = 4$ m, and generate a periodic pulse train, the power of pulse is increased with increasing the length of fiber laser with reduce its width, the nonlinear effects have a small role on the pulse power, but they effect on the modulation stability of the laser and lead to generate sideband, the behavior of the pulse converted to chaotic when increasing the frequency. [DOI: 10.1117/1.OE.53.4.046101]

Keywords: nonlinear optics; fibers laser; soliton perturbation theory; soliton amplification; fiber optics; optical fiber dispersion.

Paper 131759 received Nov. 18, 2013; revised manuscript received Jan. 22, 2014; accepted for publication Mar. 4, 2014; published online Apr. 2, 2014.

1 Introduction

The production and propagation of the pulse laser have been hot research topics in fiber optics fields in recent years,[1] where the fiber can be doped lightly with some rare-earth elements and pumped periodically to provide gain, and the properties of optics in the fibers are largely different from the pure silica fibers. This type of doped fiber is called a fiber amplifier.[2]

A fiber amplifier can be converted into a laser by placing it inside a cavity designed to provide optical feedback. Such lasers are called fiber lasers, and fiber-loop mirrors can be designed to reflect the laser light. One of these cavities is a ring cavity which is used to realize unidirectional operation of a laser. In the case of fiber lasers, an additional advantage is that a ring cavity can be made without using mirrors.[3]

Er^{+3}-doped fiber lasers can operate in several wavelength regions, one of which is 1.55-μm region. This has attracted the most attention because it coincides with the low-loss region of silica fibers used for optical communications.[4] Lasers, in general, can be classified, according to their temporal dynamics, into four principle modes of operation; namely continuous-wave (CW), Q-switched, mode-locked (ML), and Q-switched mode-locked. A CW laser generates an output optical signal with constant power. For the other cases of operation regimes, the emitted signal has a pulsed profile, characterized by parameters such as pulse duration, frequency repetition rate, pulse energy, and instantaneous peak power.[5] High-power fiber lasers have been realized from Erbium-doped fiber lasers by highly chirped picosecond pulses in a single-mode erbium-doped amplifier.[6–8] One of the most significant photonics breakthroughs in the last decade is fiber lasers consisting of a long pumped laser primarily by diode lasers directed into the fiber cladding. Average output powers from fiber lasers can reach as high as 10 kW. Fiber lasers can operate in the CW mode or in various pulse modes, even picosecond pulses.[9,10]

In one set of experiments, several diodes used to produce high pumping power, where four diode-laser bars, each emitting 45 W of power near the 915-nm wavelength, were used for pumping the fiber laser; the laser emitted up to 110 W of CW radiation at a wavelength near 1.12 μm, with an optical conversion efficiency of 58.3% (Ref. 5), optical conversion efficiency increasing to 81% by Nicholson,[11] where 55 W is produced from a high-power erbium-doped fiber laser operating at 1.555 μm, with a core pumped by a Raman fiber laser operating at 1.480 μm with 67 W of pump power.

Erbium fiber with carbon nanotubes (as saturable absorption and mode locking) are used to generate short optical pulses at a 22-MHz repetition rate with 50-kW peak power, 1.1-ps pulse width.[12] Another technique used for generating short optical pulses (at 10 kHz with 25-kW peak power, 40-ns pulse width as well as 160-kW peak power with 21-ns pulses at 1.1 kHz) is called a bulk solid-state Q-switched erbium laser.[13]

A soliton in fiber lasers is a result of the mutual nonlinear interaction among the laser gain and losses, cavity dispersion, and fiber nonlinearity, as well as the cavity effects.[14] The important question is how to generate solitons, which are affected by the gain and losses inside the laser cavity. The nonlinear Schrödinger equation supports solitons for both normal and anomalous group velocity dispersion (GVD).[15–21] The mathematical treatments for laser signal propagation in doped fiber depend on the optics signal pulse width (T) and the doped ions dipole relaxation time (T_2). When $T \leq T_2$, the rare-earth ions-doped optics fibers can be modeled by the well-known Maxwell–Bloch equation. When $T > T_2$, the description of the evolution pulse should be the Ginzburg–Landau equation.[5]

*Address all correspondence to: Younis Mohmed, E-mail: younisal_zahy72@yahoo.co.uk

0091-3286/2014/$25.00 © 2014 SPIE

A very hard task is to find exact solutions, including soliton equations, because of the changing shape of the nonlinear Schrodinger (NLS) equation according to the types of the nonlinear effects in the theoretical model, therefore one solution method will not be applicable to all equations. The hyperbolic tangent (tanh) method is a powerful technique to symbolically compute traveling wave solutions of nonlinear wave and evolution equations. In particular, the method is well suited for problems where dispersion, convection, and reaction diffusion phenomena play an important role.[22–24]

The inverse scattering transform showed that a solution to soliton equations exists.[25] Hirota developed a technique for solving soliton equations without requiring the heavy machinery of inverse scattering.[26]

Previous studies on the many new approaches for finding the exact solutions to nonlinear wave equations included the homogeneous balance method,[27,28] the hyperbolic tangent expansion method,[29,30] the trial function method,[31] the nonlinear transform method,[32] the Backlund transform,[33] the generalized Riccati equation method,[34,35] split-step Fourier method,[14] transformed rational function method,[36] and Exact 1-soliton solutions of complex-modified KdV equation with variable coefficients using solitary wave ansat.[37]

In solving problems, there are mainly two types of techniques: analytic and numerical. Analytical methods are the more rigorous ones, providing exact solutions, but they become hard to use for complex problems. Numerical methods have become popular with the development of computing capabilities, and although they give approximate solutions. The problem we have studied is finding solitary wave solutions through a core of the fiber laser, where the interaction of linear and nonlinear mechanisms makes it difficult to find general analytical solutions. In this work, we find an analytical solution for the NLS equation which describe the generating of train pulses with a high power ~650 W through Er^{+3} ring cavity length 8 m.

Our goal is to obtain a solution for the NLS equation in which include on nonlinear effects as gain dispersion , anomalous GVD, self phase modulation (SPM) and gain , by simplifying it, the method developed in this article is only applicable to pulse widths that are much longer than 100 fs for the dipole relaxation time $T \gg T_2$. We find two equations; the first equation describes the shape of laser pulse and the second equation provides the phase of the laser pulse. Section 2.1 focuses on solving equation of laser phase and Sec. 2.2 covers solution to the equation of the pulse shape. This model includes a study of the effects of SPM (Kerr effect), anomalous GVD, frequency and a small perturbations of amplitude and width of pulse on the behavior of the laser pulse during ring cavity.

2 Mathematical Analysis of the Model

The mathematical description of optical pulse propagation in a core fiber laser employs the NLS equation, and is satisfied by the pulse envelope $A(z,t)$ in the presence of gain dispersion, the losses for cavity and fiber, gain, GVD, and SPM. The amplitude $A(z,t)$ can be assumed to be real if the laser frequency ω coincides with the atomic transition frequency ω_o This equation can be written as[5]

$$i\frac{\partial A}{\partial z} = B_1\frac{\partial A}{\partial t} + \frac{1}{2}(ig_cT_2^2 + B_2^*)\frac{\partial^2 A}{\partial t^2} - \gamma|A|^2A + i(g_c - \alpha)A, \tag{1}$$

where t is the time in the rest frame, z is the propagation distance, α is total losses, including fiber, cavity and saturable absorber losses.

Note that Eq. (1) is written in the frame of reference moving with group velocity $v_g = B_1^{-1}$, transforming to a reference frame moving with the pulse and introducing the new coordinates $T = t - B_1 z$. By doing this, we eliminate the term $B_1(\partial A/\partial t)$ from the left-hand side of Eq. (1). B_2 is the GVD coefficient of the host fiber described by

$$B_2^* = \frac{d^2k}{d\omega^2} = \frac{1}{c}\left(2\frac{dn}{d\omega} + \omega\frac{d^2n}{d\omega^2}\right). \tag{2}$$

The parameter $d^2k/d\omega^2$ is associated with the refractive index. The fiber nonlinearity $\gamma = (n_2\omega/cA_{\mathrm{eff}})$ accounts for SPM effects induced by the host, ω is the carrier frequency, n_2 is the nonlinear refractive index (units m^2/W), c is the speed of light in a vacuum, and A_{eff} is the effective fiber core area. In doped fibers, the gain medium responds on a time scale much slower than that of the pulse width and realized by pumping the dopants. As a result, the saturated gain may be approximated as $g_c = g_o(1 + p_{\mathrm{ave}}/p_{\mathrm{sat}})^{-1}$, where p_{sat} is the saturation power of the gain medium, g_o is the average small-signal gain, and p_{ave} represents the average power over the cavity length L. $p_{\mathrm{ave}}/p_{\mathrm{sat}} = 0.01$ When $T_2 = 100$ fs (is doped ions dipole relaxation time),[3] $g_cT_2^2$ is a frequency-dependent gain dispersion factor. The saturable absorber is described by a simplified transfer function $\alpha = \alpha_o(1 + p_{\mathrm{ave}}/p_{\mathrm{sat}})^{-1}$.

If we make the transformation

$$\bar{\alpha} = \alpha + \alpha_o + \alpha_c,\ B_2 = B_2^* + ig_cT_2^2,\ g = g_c - \bar{\alpha}. \tag{3}$$

Equation (1) is reduced to

$$i\frac{\partial A}{\partial z} = \frac{1}{2}B_2\frac{\partial^2 A}{\partial T^2} - \gamma|A|^2A + igA. \tag{4}$$

Assume the exp-type shape of the pulse remains unchanged during propagation but allows its parameter to evolve with the propagation distance z. In this case, a suitable form of the optical field is

$$A(z,\tau) = a(z)f(\tau)e^{i\varphi}. \tag{5}$$

$a(z)$ is small perturbations of amplitude, $f(\tau)$ is the initial amplitude function to the time τ. Therefore, we can write the phase profile $\varphi(\tau,z)$ in terms of wave number $k(z)$ and carrier frequency ω of the pulse as

$$\varphi(\tau,z) = \omega\tau - k(z). \tag{6}$$

It is useful to make the transformation

$$\tau = u(z)(T - B_2\omega z), \tag{7}$$

where $u(z)$ is small perturbations of the pulse width.

By calculating $(\partial A/\partial z)$, Eq. (5) is found to satisfy

$$\frac{\partial A(z,\tau)}{\partial z}=\left[\left(i\kappa_z' a(z)+\frac{\partial a(z)}{\partial z}\right)f(\tau)+a(z)\frac{\partial f(\tau)}{\partial \tau}\frac{\partial \tau}{\partial z}\right]e^{i\varphi}, \tag{8}$$

where $\kappa_z'=dk/dz$. To find the term $d\tau/dz$ taking d/dz for Eq. (7),

$$\frac{d\tau}{dz}=\frac{du(z)}{dz}T-B_2\omega\left(u(z)+z\frac{du(z)}{dz}\right). \tag{9}$$

From Eq. (7) we get

$$T=\frac{\tau}{u(z)}+u(z)B_2\omega. \tag{10}$$

By substituting Eq. (10) into Eq. (9), pulse width is found to evolve with z as

$$\frac{d\tau}{dz}=\frac{u_z(z)'}{u(z)}\tau-u(z)B_2\omega, \tag{11}$$

where $u_z(z)'=du(z)/dz$. Substituting Eq. (11) into Eq. (8) yields

$$\begin{aligned}\frac{\partial A(z,\tau)}{\partial z}=\Bigg[&\left(i\kappa_z' a(z)+\frac{da(z)}{dz}\right)f(\tau)\\&+\left(\tau\frac{u_z(z)'}{u(z)}-u(z)B_2\omega\right)a(z)\frac{df(\tau)}{d\tau}\Bigg]e^{i\varphi}.\end{aligned} \tag{12}$$

Taking the second derivative of Eq. (5) with respect to T yields:

$$\frac{\partial^2 A(z,\tau)}{\partial T^2}=\left[2i\omega u(z)\frac{df(\tau)}{d\tau}-\omega^2 f(\tau)+u^2(z)\frac{d^2 f(\tau)}{d\tau^2}\right]a(z)e^{i\varphi}. \tag{13}$$

Substituting Eqs. (12) and (13) into Eq. (4), after some algebra, we obtain the following equation:

$$\begin{aligned}&\left(\kappa_z'+i\frac{a_z(z)'}{a(z)}-\frac{\omega^2 B_2}{2}-\gamma a(z)^2 f^2(\tau)+ig\right)f(\tau)\\&-i\tau\frac{u_z(z)'}{u(z)}\frac{df(\tau)}{d\tau}+\frac{u(z)^2 B_2}{2}\frac{d^2 f(\tau)}{d\tau^2}=0,\end{aligned} \tag{14}$$

where $a_z(z)'=da(z)/dz$ separating the real and imaginary parts of Eq. (14), we obtain the following two equations:

$$\frac{d^2 f(\tau)}{d\tau^2}+\left(\frac{2\kappa_z'}{u(z)^2 B_2}-\left(\frac{\omega}{u(z)}\right)^2-\frac{\gamma}{B_2}\left(\frac{a(z)}{u(z)}\right)^2 f(\tau)^2\right)f(\tau)=0, \tag{15}$$

$$\tau\frac{u_z(z)'}{u(z)}\frac{df(\tau)}{d\tau}+\left(\frac{a_z(z)'}{a(z)}-ga(z)\right)f(\tau)=0. \tag{16}$$

Equation (15) takes the form:

$$f''(\tau)+Qf(\tau)-\delta f(\tau)^3=0, \tag{17}$$

where

$$f_\tau''(\tau)=d^2 f(\tau)/d\tau^2,\quad \delta=\frac{\gamma}{B_2}\left(\frac{a(z)}{u(z)}\right)^2\quad\text{and}$$
$$Q=\frac{2\kappa_z'}{u(z)^2 B_2}-\left(\frac{\omega}{u(z)}\right)^2. \tag{18}$$

Equation (17) governs the pulse shape. This nonlinear equation can be solved by multiplying it by $df(\tau)/d\tau$ and integrating over τ; the result is

$$[f_\tau'(\tau)]^2+\frac{Q}{2}f(\tau)^2-\frac{\delta}{4}f(\tau)^4=C, \tag{19}$$

where C is a constant of integration. Using the boundary condition that both $f(\tau)$ and $df(\tau)/d\tau$ vanish as $\tau\to\pm\infty$, from this it follows that $C=0$.

$$[f_\tau'(\tau)]^2+\frac{Q}{2}f(\tau)^2-\frac{\delta}{4}f(\tau)^4=0. \tag{20}$$

2.1 *Phase Equation*

Finding the relation between Q and δ, and introducing a new independent variable:

$$f(\tau)=1-x^2,\ \frac{d}{d\tau}=(1-x^2)\frac{d}{dx}. \tag{21}$$

Substituting Eq. (21) into Eq. (20) yields

$$\left[(1-x^2)\frac{d}{dx}(1-x^2)\right]^2+\frac{Q}{2}(1-x^2)^2-\frac{\delta}{4}(1-x^2)^4=0. \tag{22}$$

Equating the coefficient of x^i, $i=0,1,2$, we obtain the following equation:

$$Q=1,\ \delta=-2. \tag{23}$$

Substituting Eq. (23) into Eq. (18), we get the following equations:

$$\frac{\partial\kappa}{\partial z}=\frac{B_2}{2}\omega^2-\frac{\gamma}{4}a(z)^2, \tag{24}$$

$$a(z)=\sqrt{\frac{2B_2}{\gamma}}u(z). \tag{25}$$

Taking d/dz for Eq. (25) and dividing it by Eq. (25) we get

$$\frac{a_z'(z)}{a(z)}=\frac{u_z(z)'}{u(z)}. \tag{26}$$

Multiply Eq. (16) by $f(\tau)$ and integrating with respect τ, where $\tau\to\pm\infty$ this yields

$$\frac{u_z(z)'}{u(z)}\int_{-\infty}^{\infty}\tau\frac{df(\tau)}{d\tau}f(\tau)\mathrm{d}\tau+\left(\frac{a_z(z)'}{a(z)}-\frac{g}{2}\right)\int_{-\infty}^{\infty}f^2(\tau)\mathrm{d}\tau=0 \tag{27}$$

$$\left(\frac{a_z(z)'}{a(z)}-\frac{g}{2}-\frac{1}{2}\frac{u_z(z)'}{u(z)}\right)\int_{-\infty}^{\infty}f^2(\tau)\mathrm{d}\tau=0, \tag{28}$$

since $\int_{-\infty}^{\infty}f^2(\tau)\mathrm{d}\tau\neq 0$, (represents the energy of laser pulse), we obtain the following equation:

$$\left(\frac{a_z(z)'}{a(z)}-\frac{g}{2}\right)-\frac{1}{2}\frac{u_z(z)'}{u(z)}=0. \tag{29}$$

Using Eqs. (26) and (29), we get a simple differential equation

$$\frac{a_z(z)'}{a(z)}=g. \tag{30}$$

Equation (30) can be easily integrated to obtain

$$G(z)=\frac{a(z)}{a_\circ}=e^{gz}, \tag{31}$$

where $G(z)$ is the net gain of the pulse, and z is the length of the fiber laser.

Equation (31) provides the gain coefficients representing the local gain seen by the pulse.

From Eqs. (25) and (31), the $u(z)$ is given by

$$u(z)=a_\circ\sqrt{\frac{\gamma}{2B_2}}e^{(gz)}. \tag{32}$$

Substituting Eq. (32) into Eqs. (7) and (24), we get the following equations:

$$\tau=a_\circ\sqrt{\frac{\gamma}{2B_2}}e^{(gz)}(T-B_2\omega z), \tag{33}$$

$$\frac{d\kappa}{dz}=\frac{1}{2}\left(B_2\omega^2-\frac{1}{2}\gamma a_\circ^2 e^{(2gz)}\right). \tag{34}$$

Equation (34) can be easily integrated over the length of fiber to obtain:

$$\kappa(z)=\frac{B_2}{2}\omega^2 z+\frac{\gamma a_\circ^2}{16g}(1-e^{4(gz)}). \tag{35}$$

Substituting Eqs. (33) and (35) into Eq. (6), the phase equation of the laser pulse generated through a core of fiber laser is

$$\varphi(\tau,z)=a_\circ\sqrt{\frac{\gamma}{2B_2}}e^{(gz)}\omega T-\frac{1}{2}\left(1+2a_\circ\sqrt{\frac{\gamma}{2B_2}}e^{(gz)}\right)B_2\omega^2 z-\frac{\gamma a_\circ^2}{16g}(1-e^{4(gz)}). \tag{36}$$

Equation (36) shows that the phase of the laser pulse consists of summing three parts, first a nonlinear phase shift $(\gamma a_\circ^2/16g)[1-\exp(4gz)]$, second a dispersion shift $1/2(B_2\omega^2 z)[1+2a_\circ\sqrt{\gamma/2B_2}\exp(gz)]$, and third the carrier frequency shift $a_\circ\sqrt{\gamma/2B_2}\exp(gz)\omega T$, and noting the $a_\circ\exp(gz)$ plays a dominant role to change the pulse phase.

2.2 *Pulse Amplitude Function* $\boldsymbol{A(z,T)}$

To get the amplitude function, we must investigate Eq. (20)

Substituting Eq. (23) into Eq. (20), we have that

$$[f'(\tau)]^2-\frac{1}{2}f(\tau)^2+\frac{1}{2}f(\tau)^4=0. \tag{37}$$

Hence Eq. (37) becomes

$$\int\frac{\mathrm{d}f}{f\sqrt{\frac{1}{2}(1-f^2)}}=\pm\int\mathrm{d}\tau. \tag{38}$$

If we assume a solution of the form $f(\tau)=\sec h(\theta)$, the angle θ can now be obtained by substituting it in Eq. (38). The result is found to be $\theta=\tau/\sqrt{2}$ the amplitude function becomes

$$f(\tau)=\sec h\left(\frac{\tau}{\sqrt{2}}\right). \tag{39}$$

According to Eq. (33), the parabolic (sech) solution is

$$f(\tau)=\sec h\left[\frac{a_\circ}{2}\sqrt{\frac{\gamma}{B_2}}e^{(gz)}(T-B_2\omega z)\right]. \tag{40}$$

The general solution can be obtained by substituting Eqs. (31), (36), and (40) into Eq. (5), and taking real part for $e^{i\phi}$ yields

$$\begin{aligned}A(z,T)=a_\circ\sec h&\left[\frac{a_\circ}{2}\sqrt{\frac{\gamma}{B_2}}e^{(gz)}(T-B_2\omega z)\right]\\&\times\cos\left[a_\circ\sqrt{\frac{\gamma}{2B_2}}e^{(gz)}\omega T-\frac{1}{2}\left(1+2a_\circ\sqrt{\frac{\gamma}{2B_2}}e^{(gz)}\right)\right.\\&\left.\times B_2\omega^2 z-\frac{\gamma a_\circ^2}{16g}\left(1-e^{4(gz)}\right)\right]e^{(gz)}.\end{aligned} \tag{41}$$

3 Results and Discussion

To illustrate pulse dynamics, using Eq. (41) which describes pulse laser propagation through Er^{+3} ring cavity length 8 m, we assume a (sech) input pulse has power $a_0^2=1$ W and its initial pulse width at full width at half maximum (FWHM) is $T=133$ ps $\gg T_2=0.1$ ps. Ring cavity can be designed to reflect the laser light but to transmit pump radiation and to realize unidirectional operation of a laser.[38] Six 180 W 980-nm diodes fiber were chosen for their compatibility with the input legs of available high power–tapered fiber bundle coupler technology Fig. 1 and the length of a standard single-mode fiber (SMF) was changed, therefore, the total cavity dispersion and Kerr effect were varied.[39,40]

3.1 *Output and Input Pulse Shapes*

Figure 2 shows the evolution toward a parabolic shape when a "sech" input pulse is amplified over the 8-m length of the fiber laser (a) at $z=0$ m (b) $z=8$ m comparison between the input and output pulse, we see the pulse compression where a pulse width 133 ps (FWHM) input pulse is

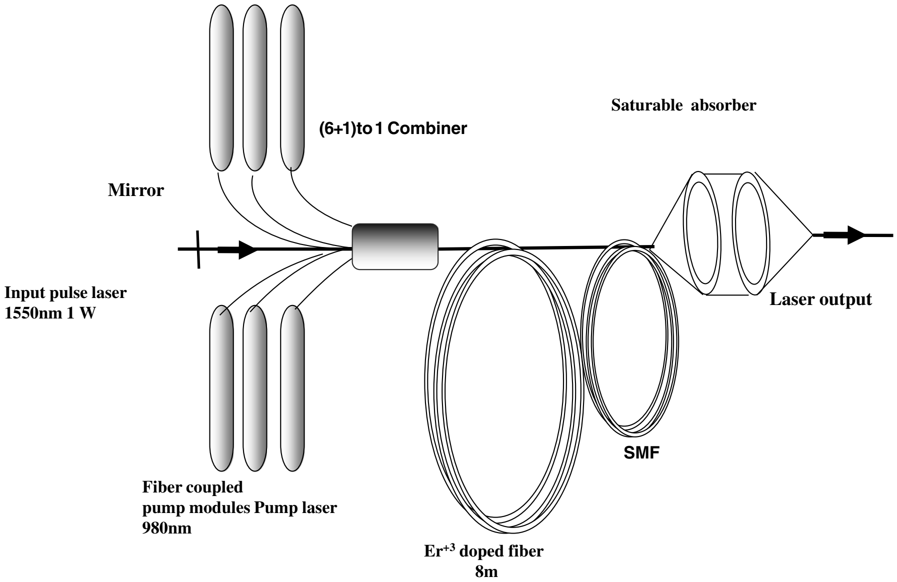

Fig. 1 Cavity arrangement for pulse generate through an erbium fiber ring laser.

compressed to 2.6 ps. The reason can be understood by noting that a pulse of most fiber lasers exhibits sidebands on both sides of the pulse and a red shift resulting from a change in the group velocity as shown Fig. 2(b). Sidebands are amplified through the gain provided by modulation instability. Modulation-instability sidebands will overlap with the origin pulse in addition, the input pulse compressed through an interplay between SPM and GVD.

3.2 *SPM Effects*

To study how SPM affects the laser pulse whose propagation in fiber laser using the parameters with the values $\gamma = 0.014$, 0.024, 0.032, and 0.056 $(\mathrm{W} \cdot \mathrm{m})^{-1}$,$B_2 = -0.044\ \mathrm{ps}^2/\mathrm{m}$, $g = 0.46\,\mathrm{m}^{-1}$, and $\omega = 1$ THz, take advantage of the values in Refs. 5, 41, and 42. Figures 3(a), 4(a), 5(a), and 6(a) show the soliton propagation in fiber laser from $z = 0$ to 4 m and the soliton amplitude increases exponentially and its width decreases exponentially in the case of $T \gg T_2$. From Figs. 3(b), 4(b), 5(b), and 6(b) one can conclude that the maximum power at $z = 8$ m has the same value 600 W, and produces a laser capable of generating a periodic pulse train. An interesting approach based on the concept of optical solutions pulses is that the pulse maintains its shape during propagation in gain fiber and the nonlinear effects in gain fiber are considered very important, because the system produces high power.

3.3 *Frequency Effects*

In this case, we discuss the variables on the behavior of the laser pulse as a result of increasing frequency as $\omega = 0.5$, 1, 2, and 3 THz for a fixed values of $\gamma = 0.056\ (\mathrm{W} \cdot \mathrm{m})^{-1}$, $B_2 = -0.044\ \mathrm{ps}^2/\mathrm{m}$, and $g = 0.46\ \mathrm{m}^{-1}$. Figures 7(a), 8(a), 9(a), and 10(a) show that the laser power grows exponentially with z and the optical pulses maintain their shape during propagation for $z = 0$ to 4 m, modulation instability can convert a soliton into a train of

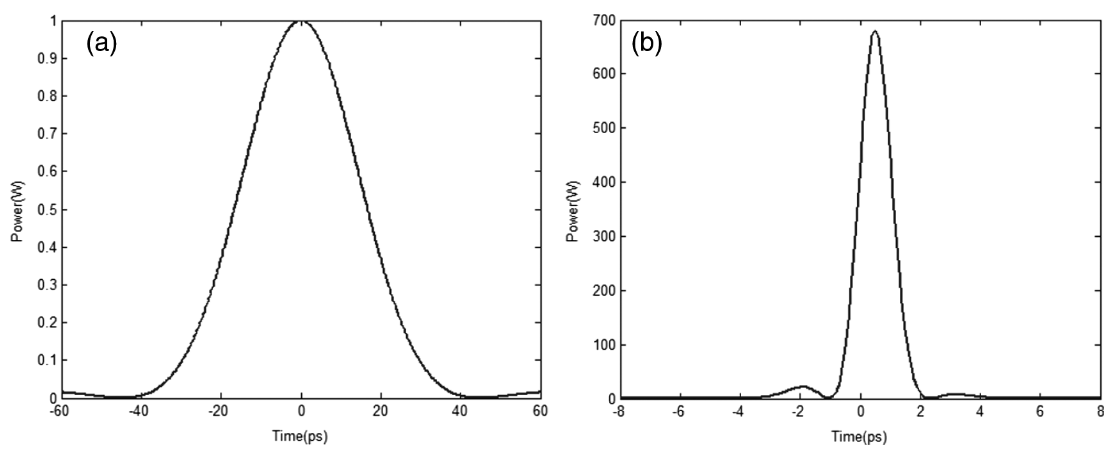

Fig. 2 The profiles of the parabolic pulse at (a) $z = 0$m (b) $z = 8$m.

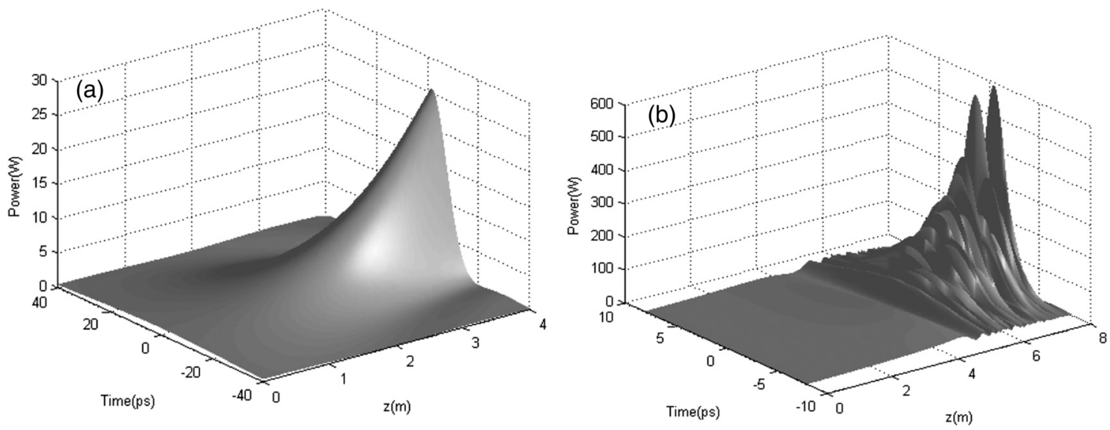

Fig. 3 Optical pulse propagation through a ring fiber laser with parameters, $\gamma = 0.014\ (\mathrm{W \cdot m})^{-1}$, $B_2 = -0.044\ \mathrm{ps^2/m}$, $g = 0.46\ \mathrm{m^{-1}}$, and $\omega = 1$ THz (a) $z = 0$ to 4 m (b)$z = 0$ to 8 m.

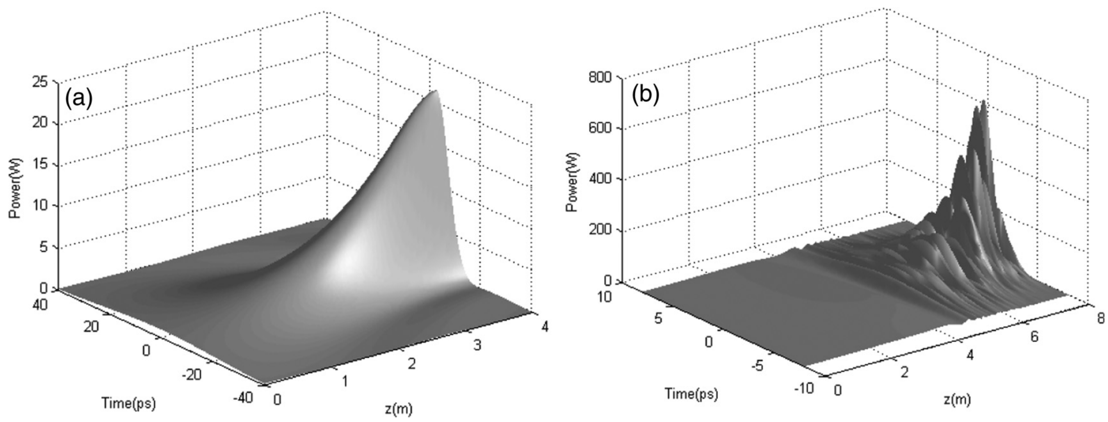

Fig. 4 Optical pulse propagation through a ring fiber laser with parameters, $\gamma = 0.024\ (\mathrm{W \cdot m})^{-1}$, $B_2 = -0.044\ \mathrm{ps^2/m}$, $g = 0.46\ \mathrm{m^{-1}}$, and $\omega = 1$ THz (a) $z = 0$ to 4 m (b) $z = 0$ to 8 m.

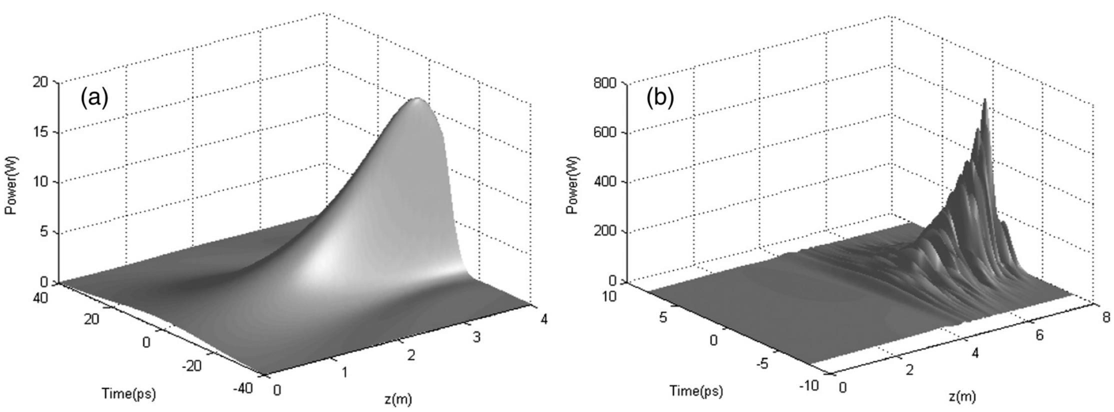

Fig. 5 Optical pulse propagation through a ring fiber laser with parameters, $\gamma = 0.032\ (\mathrm{W \cdot m})^{-1}$, $B_2 = -0.044\ \mathrm{ps^2/m}$, $g = 0.46\ \mathrm{m^{-1}}$, and $\omega = 1$ THz (a) $z = 0$ to 4 m (b) $z = 0$ to 8 m.

short pulses, the maximum power is at $z = 8$ m with a value ~600 W, the pulse width begins to broaden and chaotic behavior appears with increasing the frequency. Several mechanisms have been invoked to explain such behavior, the frequency ω dependence of the group velocity leads to pulse broadening simply because different spectral components of the pulse disperse during propagation large rapid variations in the phase and the width of the pulse can destroy a soliton if its width changes rapidly through emission of dispersive waves. Dispersive waves and solitons are resonantly amplified when $\omega = 2$ and 3 THz, and such a resonance can lead to unstable and chaotic behavior as shown in Figs. 7(b), 8(b), 9(b), and 10(b).[43]

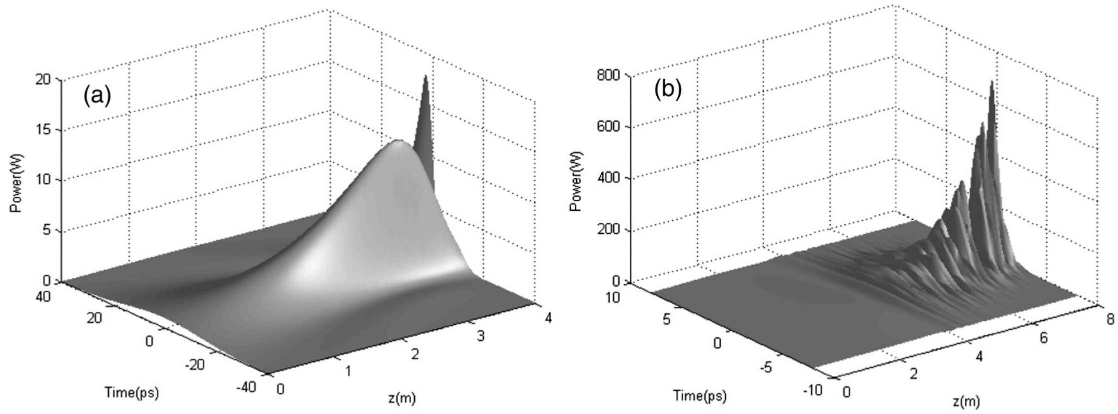

Fig. 6 Optical pulse propagation through a ring fiber laser with parameters, $\gamma = 0.056\ (\mathrm{W \cdot m})^{-1}$, $B_2 = -0.044\ \mathrm{ps^2/m}$, $g = 0.46\ \mathrm{m^{-1}}$, and $\omega = 1$ THz (a) $z = 0$ to 4 m (b) $z = 0$ to 8 m.

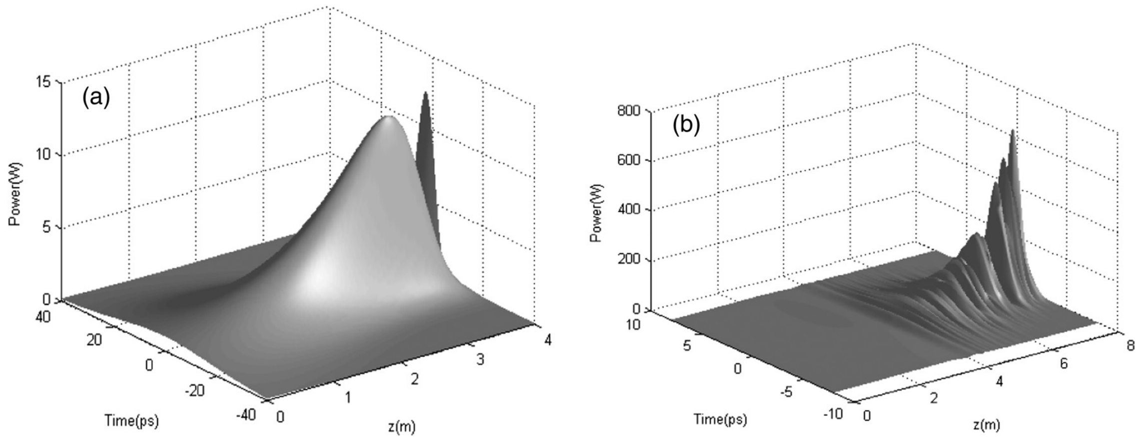

Fig. 7 Optical pulse propagation through a ring fiber laser with parameters, $\gamma = 0.056\ (\mathrm{W \cdot m})^{-1}$, $B_2 = -0.044\ \mathrm{ps^2/m}$, $g = 0.46\ \mathrm{m^{-1}}$, and $\omega = 0.5$ THz (a) $z = 0$ to 4 m (b) $z = 0$ to 8 m.

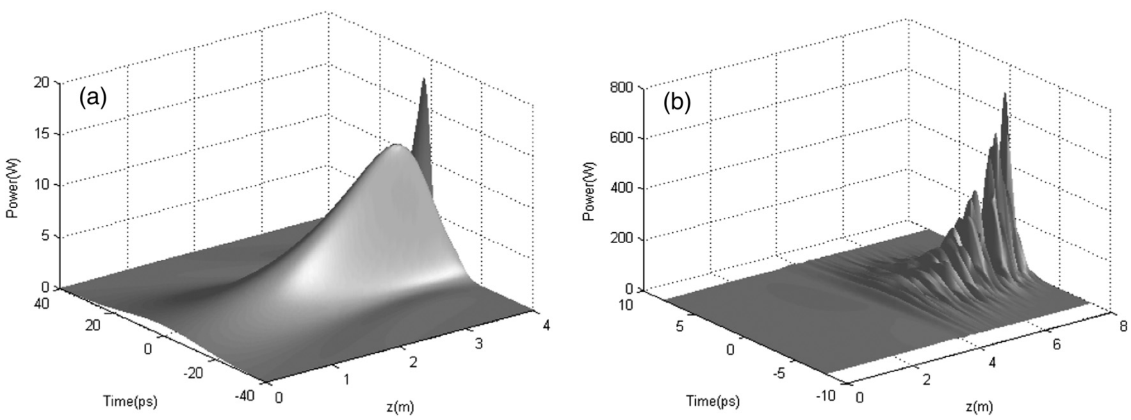

Fig. 8 Optical pulse propagation through a ring fiber laser with parameters $\gamma = 0.056\ (\mathrm{W \cdot m})^{-1}$, $B_2 = -0.044\ \mathrm{ps^2/m}$, g $= 0.46\ \mathrm{m^{-1}}$, and $\omega = 1$ THz (a) $z = 0$ to 4 m (b) $z = 0$ to 8 m.

3.4 *Anomalous Group Velocity GVD Effects*

An important question that we can answer with our model is how the anomalous GVD affects the behavior of the pulse propagation in fiber laser. When values of B_2 varies (-0.012, -0.023, and -0.035) $\mathrm{Ps^2/m}$ and, $\gamma = 0.056\ (\mathrm{W \cdot m})^{-1}$, $g = 0.46\ \mathrm{m^{-1}}$, and $\omega = 1$ THz. The results show solitons can still form if the SPM effects are balanced by the average dispersion and become stable during the first 4 m as shown in Figs. 11(a), 12(a), and 13(a). It is found that the dispersion induced broadening of the laser pulse and this leads to

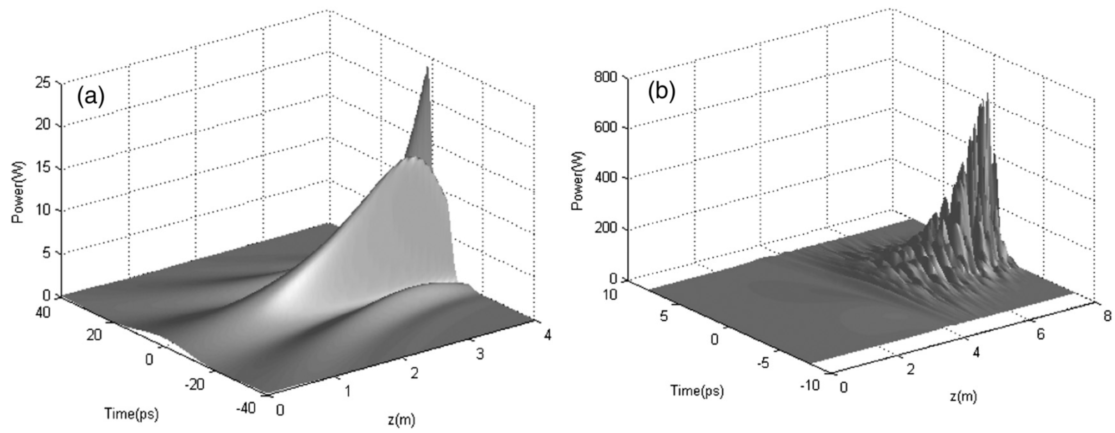

Fig. 9 Optical pulse propagation through a ring fiber laser with parameters, $\gamma = 0.056$ $(\mathrm{W \cdot m})^{-1}$, $B_2 = -0.044$ ps^2/m, $g = 0.46$ m^{-1}, and $\omega = 2$ THz (a) $z = 0$ to 4 m (b) $z = 0$ to 8 m.

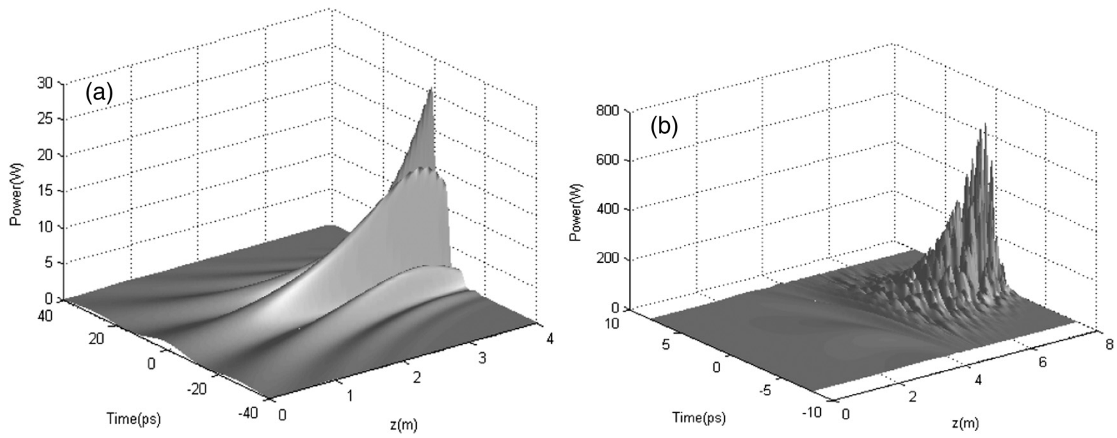

Fig. 10 Optical pulse propagation through a ring fiber laser with parameters, $\gamma = 0.056$ $(\mathrm{W \cdot m})^{-1}$, $B_2 = -0.044$ ps^2/m, $g = 0.46$ m^{-1}, and $\omega = 3$ THz (a) $z = 0$ to 4 m (b) $z = 0$ to 8 m.

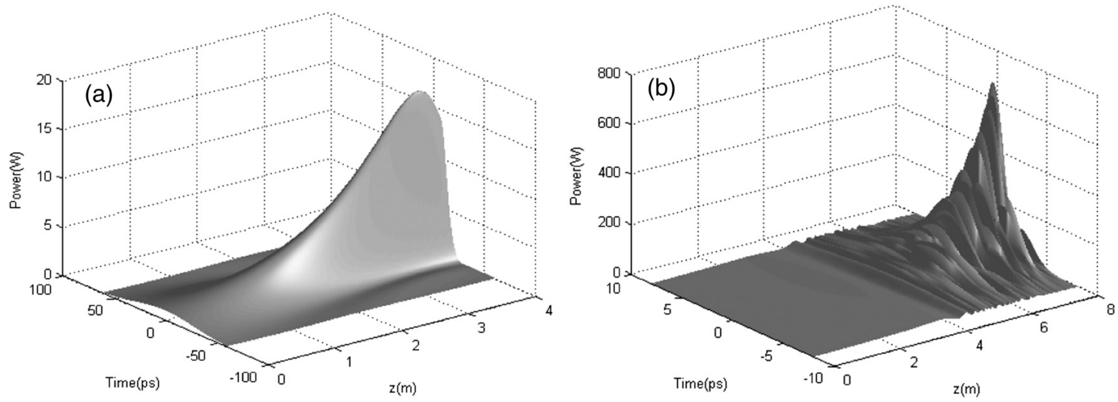

Fig. 11 Optical pulse propagation through a ring fiber laser with parameters, $\gamma = 0.056$ $(\mathrm{W \cdot m})^{-1}$, $B_2 = -0.012$ ps^2/m, $g = 0.46$ m^{-1}, and $\omega = 1$ THz (a) $z = 0$ to 4 m (b) $z = 0$ to 8 m.

a reduction in the power with increasing the dispersion. The dispersion effect is small on the shape of the pulse because the cavity length is short, 8 m. The SPM $(\gamma a_\circ^2/16g)[1-\exp(4gz)]$ became quite significant at higher power levels, therefore solitons result from a balance between anomalous GVD and SPM. Figures 11(b), 12(b), and 13(b) show the solitons can become unstable in the presence of GVD and break up into a train of short pulses at a width (FWHM) 2.6 ps.

Our analytical solution shows that the phase of the laser pulse depends on a nonlinear phase shift $(\gamma a_\circ^2/16g)\times[1-\exp(4gz)]$, dispersion shift $a_\circ\sqrt{\gamma/2B_2}\exp(gz)\omega T$ and the

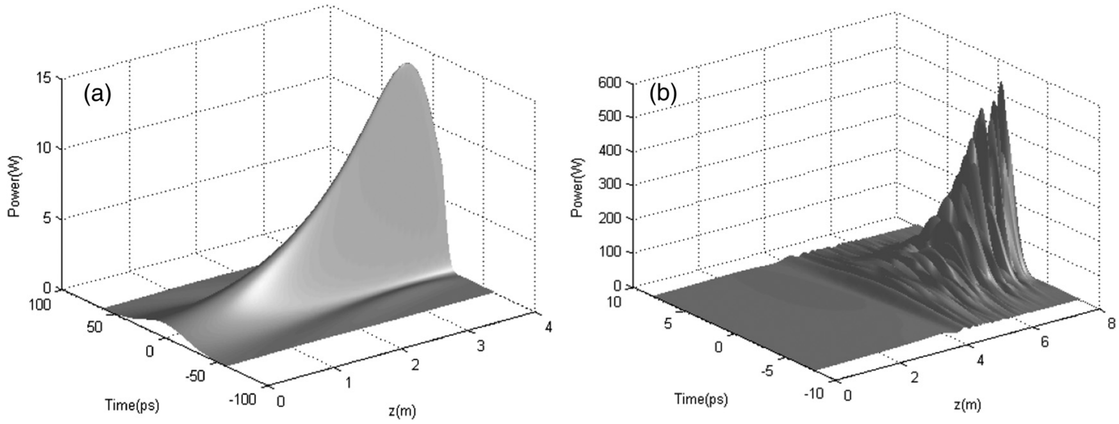

Fig. 12 Optical pulse propagation through a ring fiber laser with parameters, $\gamma = 0.056\ (\mathrm{W \cdot m})^{-1}$, $B_2 = -0.023\ \mathrm{ps^2/m}$, $g = 0.46\ \mathrm{m^{-1}}$, and $\omega = 1$ THz (a) $z = 0$ to 4 m (b) $z = 0$ to 8 m.

carrier frequency shift $1/2(B_2\omega^2 z)[1+2a_\circ\sqrt{\gamma/2B_2}\exp(gz)]$. As a result, the gain coefficients play a dominant role to change the pulse phase.

3.5 *Gain Effects*

A new feature is that the parameter g plays an important role in determining the properties of the pulse. Figure 14(a) shows the behavior of the pulse for net gain $g = 0.1\ \mathrm{m^{-1}}$ with the parameters $\gamma = 0.056\ (\mathrm{W \cdot m})^{-1}$, $B_2 = -0.044\ \mathrm{ps^2/m}$ and $\omega = 1$ THz. An important property of optical solitons is that they are remarkably stable against small perturbations $a(z)$ and $u(z)$. Physically, this behavior can be understood by noting that a soliton results from a balance between GVD and SPM. In this case, the net gain is small compared with the other cases. Therefore, the perturbations are weak, $a(z) = a_\circ e^{gz}$ and $u(z) = a_\circ\sqrt{\gamma/2B_2}e^{(gz)}$,and the power of soliton exponentially increased with increasing the length of fiber laser beginning from 1 to 6.3 W at $z = 8$ m.

Input pulse width 133 ps (FWHM) compressed to 66.8 ps because of the combination of anomalous GVD and SPM that leads to soliton-effect compression and nonlinear effects (anomalous GVD and SPM) play an important role in this case as shown in Figs. 14(b) and 14(c).

3.6 *Comparing the Analytical Results with Numerical Methods*

Our results in regards to the parabolic shape of pulse Fig. (2) and the behavior of the laser pulse have good agreement with the results in Refs. 42 to 46. Comparing our analytical method with a numerical method as split-step Fourier method SSFM, it is important to understand the accuracy and stability of the SSFM algorithm. Indeed, the step sizes in z and t must be selected carefully to maintain the required accuracy of calculation, depending on the order of the method used. There are many approximations in split-step Fourier method SSFM. As an example, when using the Baker–Hausdorff formula, the third order in h is neglected. The loss operator is left out for simplicity. Ignoring the third order terms and higher when using Taylor expansion, the solution of Modified NLS and Maxwell–Bloch equation (which describes the dynamic response of a two-level system of optical amplifier and fiber laser) is more accurate, however, we should bear in mind that it is only applicable to the lower gain regime

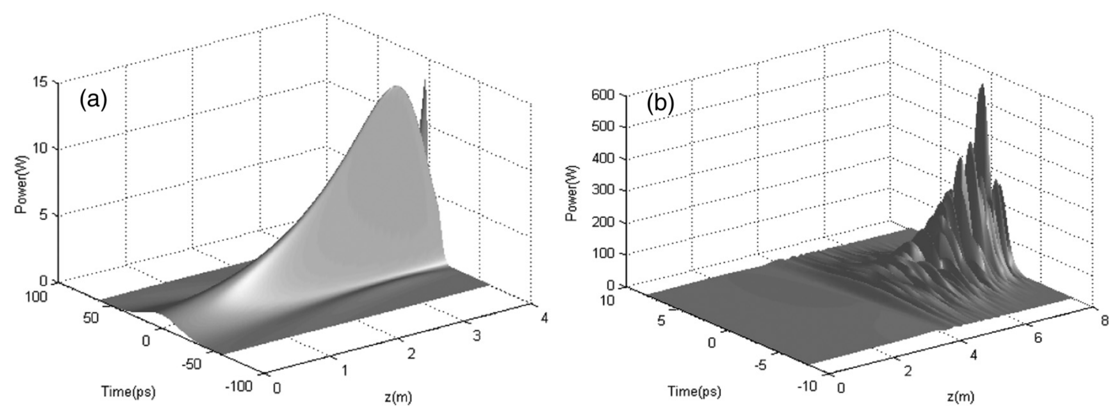

Fig. 13 Optical pulse propagation through a ring fiber laser with parameters, $\gamma = 0.056\ (\mathrm{W \cdot m})^{-1}$, $B_2 = -0.035\ \mathrm{ps^2/m}$, $g = 0.46\ \mathrm{m^{-1}}$, and $\omega = 1$ THz (a) $z = 0$ to 4 m (b) $z = 0$ to 8 m.

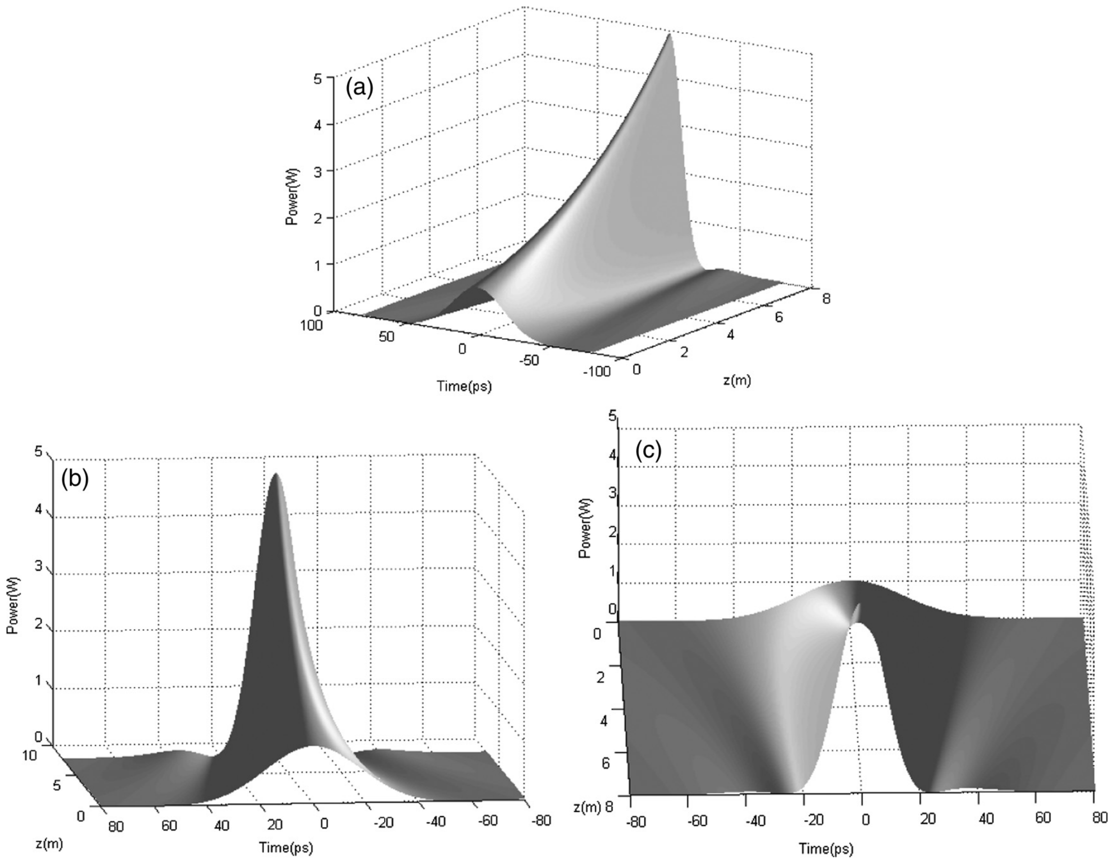

Fig. 14 (a) Optical pulse propagation through a ring fiber laser. (b) Shape of the input pulse. (c) Shape of the output pulse with parameters, $\gamma = 0.056\ (\mathrm{W} \cdot \mathrm{m})^{-1}$, $B_2 = -0.044\ \mathrm{ps}^2/\mathrm{m}$, $g = 0.1\ \mathrm{m}^{-1}$, and $\omega = 1$ THz.

$G = 20$ dB. In addition, this equation must be solved for pulses whose width is shorter or comparable with the dipole relaxation time ($T_2 < 0.1$ ps). The solution becomes invalid under the condition $T \gg T_2$.

4 Conclusions

By applying our technique to the NLS equation included nonlinear optics as gain dispersion, anomalous GVD, SPM, and gain, we have derived two differential equations for the shape of the pulse and the phase. At high-level net gain, solution of the equation plays the role to generate a train pulse with (sech) shape through the fiber laser. We have two periods to solution; the first $z = 0$ to 4 m, the pulse shape does not change and the second $z = 4$ to 8 m, the modulation instability can convert a pulse into a train of short pulses. It is evident that GVD and SPM play a major role in establishing pulse train at a high-power level. In our model, at $T \gg T_2$, the power was large enough to lead to considerable pulse narrowing during the amplification process, and it provides an important reference for experimental research on optical pulse in fiber lasers.

Acknowledgments

The author is grateful for the assistance of prof. Dr. Alexander Pisarchik Ass. Prof. Dr. Kais Al-Naimee Mr. Hameed Mahood, and Ms. Leili Masoudnia.

References

1. M. E. Fermann et al., "Self-similar propagation and amplification of parabolic pulse in optical fibers," *Phys. Rev. Lett.* **84**(26), 6010–6013 (2000).
2. C. Finot et al., "Parabolic pulse evolution in normally dispersive fiber amplifiers preceding the similariton formation regime," *Opt. Express* **14**(8), 3161–3170 (2006).
3. T. M. Shay and F. J. Duarte, "*Tunable Laser Applications*," Brian J. Thompson, Ed., p. 179, CRC Press Taylor and Francis Group, USA (2013).
4. M. J. F. Digonnet, *Rare-Earth Doped Fiber Lasers and Amplifiers*, Michel J. F Dionnet, Ed., p. 323, Marcel Dekker Inc., New York (1993).
5. G. P. Agrawal, *Application of Nonlinear Fiber Optics*, P. L. Kelley, I. P. Kamnow, and G. P. Agrawal, Eds., p. 170, Academic Press, USA (2001).
6. J. W. Nicholson and A. Yablon, "A high power, single-mode, erbium-doped fiber amplifier generating 30 fs pulses with 160 kW peak power," in *Lasers and Electro-Optics, 2004*, Vol. 1(2), pp. 1–2 (2004).
7. J. W. Nicholson et al., "High-power single-mode all-fiber femtosecond laser system and its use in continuum generation," *Proc. SPIE* **5662**, 373–377 (2004).
8. A. Zhang et al., "Temporal characteristics of a high-power erbium-doped fiber ring laser," *Proc. SPIE* **7134**, 713407 (2008).
9. P. Polynkin et al., "All-fiber picosecond laser system at 1.5 μm based on amplification in short and heavily doped phosphate-glass fiber," *IEEE Photonics Technol. Lett.* **18**(21), 2194–2196 (2006).
10. C. J. S. De Matos et al., "20-kW peak power all-fiber 1.57 μm source based on compression in air-core photonic band gap fiber, its frequency doubling, and broadband generation from 430 to 1450 nm," *Opt. Lett.* **30**(4), 436–438 (2005).
11. J. W. Nicholson, "High-power continuous wave erbium-doped fiber laser pumped by a 1480-nm Raman fiber laser," *Proc. SPIE* **8237**, 82370K (2012).
12. J. Jasaparal et al., "Simultaneous amplification and compression of picosecond pulses to 50 kW in Er fiber," in *Lasers Electro-Opt. CLEOE-IQEC*, pp. 1–1 (2007).

13. S. D. Setzler et al., "High-peak-power erbium lasers resonantly pumped by fiber lasers," *Proc. SPIE* **5332**, 85–96 (2004).
14. D. Y. Tang et al., "Compound pulse solitons in a fiber ring laser," *Phys. Rev. A* **68**(1), 013816–1 (2003).
15. J. Wu et al., "Soliton polarization dynamics in fiber lasers passively mode-locked by the nonlinear polarization rotation technique," *Phys. Rev. E* **74**(4), 046605 (2006).
16. F. Parmigiani et al., "Ultra-flat SPM-broadened spectra in a highly nonlinear fiber using parabolic pulses formed in a fiber Bragg grating," *Opt. Express* **14**(17), 7617–7622 (2006).
17. D. Méchin et al., "Experimental demonstration of similariton pulse compression in a comb like dispersion decreasing fiber amplifier," *Opt. Lett.* **31**(14), 2106–2108 (2006).
18. V. I. Kruglov, A. C. Peacock, and J. D. Harvey, "Asymptotically exact parabolic solutions of the generalized nonlinear Schrödinger equation with varying parameters," *Opt. Soc. Am.* **23**(12), 2541–2550 (2006).
19. F. O. Ilday et al., "Self-similar evolution of parabolic pulse in a laser," *Phys. Rev. Lett.* **92**(21), 213902–1 (2004).
20. V. I. Kruglov, A. C. Peacock, and J. D. Harvey, "Exact self-similar solutions of the generalized nonlinear Schrödinger equation with distributed coefficients," *Phys. Rev. Lett.* **90**(11), 113902 (2003).
21. C. K. Nielsen et al., "Self-starting self similar all-polarization maintaining Yb-doped fiber laser," *Opt. Express* **13**(23), 9346–9351 (2005).
22. G. P. Agrawal, *Nonlinear Fiber Optics*, P. L. Christiansen, M. P. Sorensen, and A. C. Scott, Eds., p. 129, Elsevier, San Diego (1995).
23. M. A. Abdou, "The extended tanh-method and its applications for solving nonlinear physical models," *Appl. Math. Comput.* **190**(1), 988–996 (2007).
24. S. A. El-Wakil and M. A. Abdou, "Modified extended tanh function method for solving nonlinear partial differential equations," *Chaos, Solitons Fractals* **31**, 1256–1264 (2007).
25. R. Hirota and J. Satsuma, "Soliton solution of a coupled KdV equation," *Phys. Lett. A.* **85**(8–9), 407–408 (1981).
26. M. J. Ablowitz and P. A. Clarkson, *Solitons, Nonlinear Evolution Equations and Inverse Scattering Transform*, J. W. S. Cassels, Ed., p. 131, Cambridge University Press, Cambridge (1991).
27. M. L. Wang, "Solitary wave solutions for variant Boussinesq equations," *Phys. Lett. A.* **199**(3–4), 169–172 (1995).
28. E. M. E. Zayed, H. A. Zedan, and K. A. Gepreel, "On the solitary wave solutions for nonlinear Hirota-Satsuma coupled KdV equations," *Chaos, Solitons Fractals* **22**, 285–303 (2004).
29. L. Yang, J. Liu, and K. Yang, "Exact solutions of nonlinear PDE nonlinear transformations and reduction of nonlinear PDE to a quadrature," *Phys. Lett. A* **278**, 267–270 (2001).
30. E. M. E. Zayed, H. A. Zedan, and K. A. Gepreel, "Group analysis and modified tanh-function to find the invariant solutions and soliton solution for nonlinear Euler equations," *J. Nonlinear Sci. Numer. Simul.* **5**(3), 221–234 (2004).
31. M. Inc and D. J. Evans, "On travelling wave solutions of some nonlinear evolution equations," *J. Comput. Math.* **81**(2), 191–202 (2004).
32. J. L. Hu, "A new method of exact travelling wave solution for coupled nonlinear differential equations," *Phys. Lett. A*322(3–4), 211–216 (2004).
33. C. Rogers and W. F. Shadwick, *Backlund Transformations*, D. G. Crighton, Ed., p. 67, Cambridge University Press, New York (1982).
34. Z. Y. Yan and H. Q. Zhang, "New explicit solitary wave solutions and periodic wave solutions for Whitham-Broer-Kaup equation in shallow water," *Phys. Lett. A* **285**(5–6), 355–362 (2001).
35. A. V. Porubov, "Periodical solution to the nonlinear dissipative equation for surface waves in a convecting liquid layer," *Phys. Lett. A* **221**(6), 391–394 (1996).
36. W. X. Ma and J. H. Lee Chand, "A transformed rational function method and exact solutions to the $(3+1)$ dimensional Jimbo Miwa equation," *Chaos, Solitons Fractals* **42**(3), 1356–1363 (2009).
37. H. Kumar and F. Chand, "Soliton solutions of complex modified KdV equation with time-dependent coefficients," *Indian J. Phys.* **87**(9), 909–912 (2013).
38. V. Mikirtychev, *Fundamentals of Fiber Lasers and Fiber Amplifiers*, W. T. Rhodes Ed., p. 96, Springer, USA (2014).
39. C. Vinegoni, M. Wegmuller, and N. Gisin, "Measurements of the nonlinear coefficient of standard SMF, DSF, and DCF fibers using a self-aligned interferometer and a Faraday Mirror," *IEEE Photonics Technol. Lett.* **13**(12), 1337–1339 (2001).
40. M. Faucher et al., "High power monolithically integrated all-fiber laser design using single-chip multimode pumps for high reliability operation," *Proc. SPIE* **6873**, 68731T (2008).
41. N. G. Usechak and G. P. Agrawal, "Semi-analytic technique for analyzing mode-locked lasers," *Opt. Express* **13**(6), 2075–2081 (2005).
42. F. Jiel et al., "Analytic solutions of self-similar pulse based on Ginzburg-Landau equation with constant coefficients," *China Ser. G-Phys. Mech. Astron.* **51** (3), 299–306 (2008).
43. A. N. Pisarchik et al., "Rogue waves in a multistable fiber laser," *Phys. Rev. Lett.* **107**, 274101 (2011).
44. K. Sergei Turitsyn, "Dispersion managed solitons fiber systems and lasers," *J. Phys. Rep.* **521**(4), 135–203 (2012).
45. J. R. Costa and C. R. Paiva, "Modified split-step Fourier method for the numerical simulation of soliton amplification in erbium-doped fibers with forward propag-ating noise," *IEEE J. Quantum Electron.* **37**(1), 145–151 (2001).
46. I. A. Yarutkina et al., "Numerical modeling of fiber lasers with long and ultra-long ring cavity," *Opt. Express* **21**(10), 12942–12950 (2013).

Younis Mohamed Atiah Al-zahy is an associate professor of physics in the Department of Science at Misan University since 2006. He received a PhD and MSc degrees in the College of Physical Science from Al- Mustansiriya University (IRAQ) in 2006 and 1998 res. Currently, he works at the Laboratory of Laser Technology, and the College of science as lecturer in physics. He has published many papers in fields of fiber lasers.